

# Study of the Performance of a Solar Refrigerator Using a Silica Gel-water Combination

## Abstract:

Solar adsorption refrigeration as an environmentally-friendly refrigeration method has attracted a great deal of interest over the world. This technology will therefore benefit developing countries with high solar energy potential. The aim of this work is to contribute to a better understanding of the functioning of the refrigeration systems by adsorption. An experimental survey is conducted on such a prototype using silicagel-water couple constructs by BLM and installed in Ouagadougou (IRSAT) in the eighties. In this study, we measured the overall solar radiation on the collector, ambient temperature and the temperature of the various parts of the system, i.e., the collector, condenser and evaporator. We then used A. Errougani's correlation to estimate the mass of water adsorbed to calculate the amount of cold produced at the evaporator. The observed facts were that the SCOP of this machine varies between 0,091 and 0,138 for an average daily solar radiation ranging from 14,56 MJ and 18,68 MJ. This prototype, despite its old age had an interesting SCOP and testifies an increase of the temperature to the evaporator in relation to the one predicted initially.

**Keywords:** Adsorption, Refrigeration, Silicagel-water, solar energy, Solar performance coefficient, experimental.

## Introduction

Usually, cold is obtained using compression systems, which require enormous amounts of energy to operate [1]. These systems use refrigerants such as hydrofluorocarbons (HFCs), hydrochlorofluorocarbons (HCFCs) and hydrofluorocarbons (HFCs), which are responsible for ozone depletion [2]. As a result, these systems contribute to climate change through the combined action of refrigerant emissions and the increase in greenhouse gas emissions.

In this context, adsorption refrigeration systems are a good alternative because they produce cold using renewable energy sources, particularly solar energy. In addition to being a simple technology, adsorption refrigeration systems offer an alternative solution for both the environment and the countries with high levels of sunshine. However, these adsorption refrigeration systems have been the subject of intense research over the last decade, and prototypes have been designed [1],[3],[4] among which we have :

Boubakri et al. [5] designed a solar adsorption refrigeration system using a tubular adsorber-collector operating with activated carbon-methanol. This prototype was tested under meteorological conditions in Agadir (Morocco). It achieved evaporator temperatures of  $-6^{\circ}\text{C}$ .

Their experimental results showed that the solar coefficient of performance (SCOP) varied between 0.08 and 0.12.

In Switzerland, Hildbrand et al. have developed a prototype solar refrigerator based on the silica gel-water couple, using a single-glazed flat-plate solar collector [6]. This adsorber-collector features ventilation flaps that allow night-time cooling and promote adsorption. This cooling system performed well, with a coefficient of performance (SCOP) of 0.16.

Bouzeffour et al. [7] developed and tested a solar refrigeration system with the adsorption process operating with the silicagel-water couple. Their prototype uses a single-glazed flat-plate solar collector. The minimum temperature reached in the evaporator is around +5°C. The experimental solar coefficient of performance (SCOP) obtained with the prototype during the test period ranged from 0.083 to 0.09 under the climatic conditions of Bou-Ismaïl (Algeria).

G.C.Tubremouya et al.[8] have carried out an experimental analysis of the operation of a solar adsorption refrigerator designed to preserve pharmaceutical products and installed in Yako (Burkina Faso). This device uses zeolite/water as the working couple. The study consisted in measuring the solar radiation incident on the adsorber-collector, the temperature of all components of the adsorber-collector, the condenser, the evaporator and the storage tank. The results show that the minimum temperature reached by the evaporator was 4°C, and the solar adsorption refrigerator can provide a solar coefficient of performance ranging from 0.09 to 0.185 under total solar radiation of 19 MJ/m<sup>2</sup>. From these results, this study demonstrated the technical feasibility of the solar adsorption refrigerator prototype. In view of their environmental benefits and the match between cooling demand and solar radiation, several researchers are focusing their research on solar adsorption refrigerators.

This article presents the actual operation of a solar adsorption refrigerator using the silicagel/water couple under the climatic conditions of Ouagadougou. The aim of the present work is to contribute to a better understanding of the operation of adsorption refrigeration systems through an experimental study of the Brissoneau and Lotz-Marine (BLM) prototype.

## **1. Material and methods**

### **1.1. Study area**

The prototype under study is located in Burkina Faso (Ouagadougou) at latitude 12°22'30.3" and longitude 01°29'53.31". Manufactured by the Brissoneau and Lotz-Marine (BLM) laboratory, comprises two sensor-adsorbers, a condenser and an evaporator housed in the

refrigeration chamber. Temperature and solar radiation measurements were carried out in June and July. In this period, the sky is less charged with dust particles in Ouagadougou.



Figure 1: Photo of the adsorption solar refrigerator

### 1.2. Solar refrigerator working principle

This system operates on an intermittent cycle basis. The intermittency of the solar adsorption refrigerator's cold production cycle is synchronized with that of the solar energy source. The operating principle of these system is based on the thermodynamic cycle (Figure 2), which can be summarized as follows [9]:

- Heating phase during the day

From 1 to 2 (isosteric heating), the adsorber is insulated. Under the effect to heat, the pressure and temperature of the mixture increase, while the total mass of refrigerant adsorbed remains constant and equal to  $m_{max}$ . This pressurization phase ends as soon as the pressure equals that in the condenser  $P_c$  (point 2), where  $P_c = P_s(T_c)$ .

From 2 to 3 (desorption-condensation), the adsorber is brought into contact with the condenser and refrigerant desorption begins. The adsorber is now at a pressure equal to the condensation pressure, and follows the isobaric pressure imposed by the condenser. As heating continues, the temperature of the mixture in the adsorber will rise to the maximum temperature  $T_g$ .

- Cooling phase at night

From 3 to 4 (isostere), the adsorber is isolated again. Cooling of the adsorbent/adsorbate mixture begins at point 3, where temperature and pressure decrease until the pressure is equals to what is in the evaporator  $P_e = P_s(T_e)$ . The temperature reached is known as the adsorption

"threshold temperature"  $T_{c2}$  (point 4). The total mass of fluid adsorbed is constant at this stage, equal to  $m_{min}$ .

From 4 to 1 (adsorption-evaporation), the adsorber is connected to the evaporator. The steam produced is absorbed back into the adsorber, until the temperature of the adsorbent/adsorbate mixture reaches a minimum  $T_1$ . The system then follows the isobaric pressure imposed by the evaporator, which corresponds to the saturation pressure of the refrigerant at evaporation temperature. At this point, the machine is ready to start a new cycle.

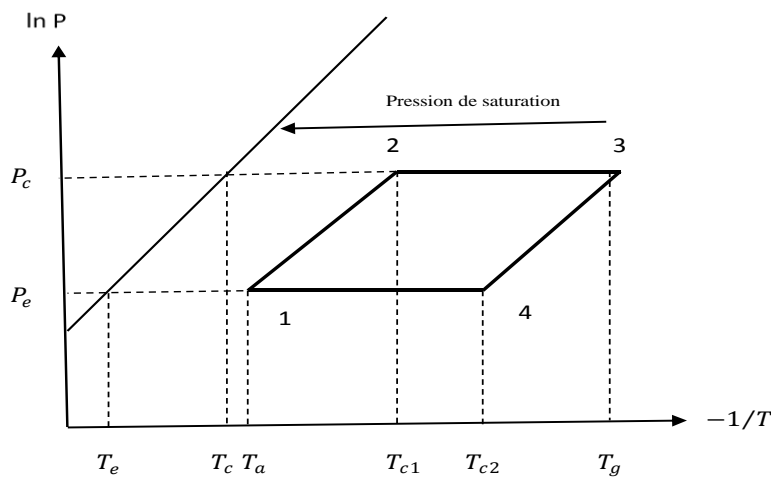


Figure 2: Ideal cycle of an adsorption Solar refrigerator

### 1.3. Experimental protocol

The study of the adsorption solar refrigerator requires knowledge of data such as the temperature of its various parts and the amount of sunshine. For temperature measurement, K-type thermocouples are used with an accuracy of one percent (1%). The pyranometer type "sensor basic including irradiance sensor and module temperature sensor" is also used. K-type thermocouples are placed on each of the parts, and a pyranometer is placed on the glass at the same angle as the glass. All are then connected to a data logger, enabling data to be recorded automatically over a five-second time interval. The data collection diagram is illustrated in Figure 3.

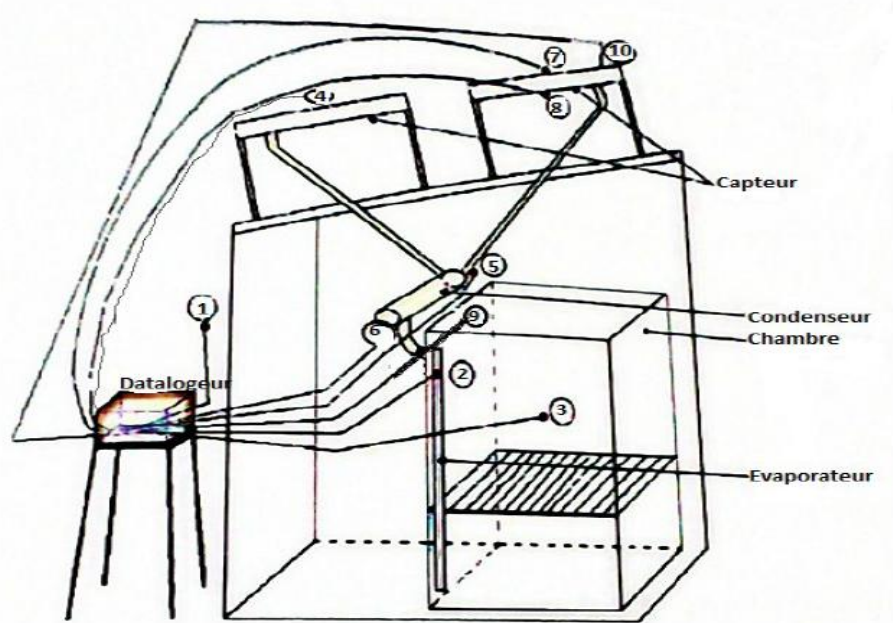


Figure 3: Experimental setup

#### 1.4.Uncertainty analysis

The experiment have been conducted through with high level precaution, however errors did crept into the measurement of various parameters. This can happen because of the large number of instruments used in the experiment. As a result, it is believed that measurement inaccuracy is possible during experimental work. Total measurement uncertainty is defined as the difference between the quantity measured and its value. The uncertainty analysis performed by Kline and McClintock was used to estimate the uncertainty associated with the present study. Consequently, the uncertainty analysis was carried out using the experimental results obtained from the present study. The error values of various parameters for the present experimental work are given in the table.

Table 1. The measures, symbols and Uncertainty.

N°	Measure	Symbol	uncertainty
1	Ambient temperature	$T_{amb}$ [°C]	$\pm 1.5$
2	Sensor temperature	$T_{cap}$ [°C]	$\pm 2.6$
3	Condenser temperature	$T_c$ [°C]	$\pm 1.95$
4	Evaporator temperature	$T_e$ [°C]	$\pm 3.23$
5	Solar radiation	$I_g$ [ $W/m^2$ ]	$\pm 0.38$

### 1.5. Solar coefficient of performance calculation (SCOP)

The coefficient of solar performance SCOP of the adsorption solar refrigerator studied is given by the following relationship:

$$SCOP = \frac{Q_f}{I_g}$$

$I_g$  : is the solar energy received by the collector-adsorber.

$$I_g = A * \int_{t_l}^{t_s} I(t) dt$$

A: collector area in  $m^2$ ;

I(t): hourly solar irradiance in  $W/m^2$

$Q_f$  : is the amount of heat extracted from the evaporator:

$$Q_f = m_{ad} [L(T_e) - C_{pa} (T_c - T_e)]$$

As, the prototype studied does not have a device for measuring condensate mass. A. Erroungani's correlation was used to estimate the mass of water adsorbed  $m_{ad}$ . This correlation is given by the relation [4]:

$$\log(m_{ad}) = 2,44859 \log\left(\frac{I_g}{T_{amb}}\right) - 4,08861$$

## 2. Results and discussion

### 2.1. Solar radiation

Figure 4 illustrates variations in solar radiation over three days as a function of time on the site of experience. The figure shows that solar radiation begins to increase at sunrise, reaching its maximum value between 576.45 and 733.38  $W/m^2$  in the middle of the day between 11am and 1pm; and then decreases beyond this period to reach zero around 6pm. The low level of sunshine in the middle of the day on 01/07/2017 is linked to the passage of thunderstorms.

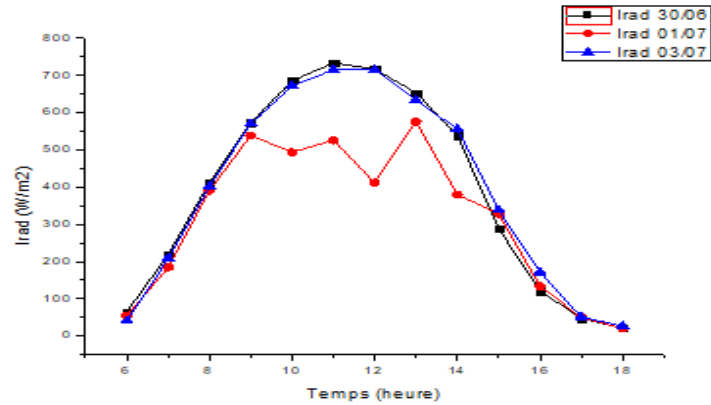


Figure 4: Evolution of solar radiation

## 2.2. Temperature profile in the collector

Figure 5 illustrates the evolution of solar collector temperature as a function of time for different test days. It can be seen that the temperature profile follows the same pattern as solar radiation. The maximum collector temperature values obtained range from 67.13°C to 78°C for these test days. The collector temperature remained constant throughout the heating period from 11am to 1pm. After the temperature peak, there was a gradual drop in collector temperature as radiation levels fell.

A similar trend in sensor temperature evolution was observed by author F. Bouzeffour [3]. A maximum temperature values obtained in the adsorbent bed range from 100°C to 119°C. Moreover, the maximum temperature of the adsorbent bed remained constant during the heating period from 12:00 to 14:00, corresponding to the maximum intensity of solar radiation. It should be noted, that the maximum temperature values within F. Bouzeffour's [3] adsorbent bed were higher than those obtained in our study. This suggests that the reflective surface is conducive to higher temperatures in the adsorbent bed in F. Bouzeffour's [3] study.

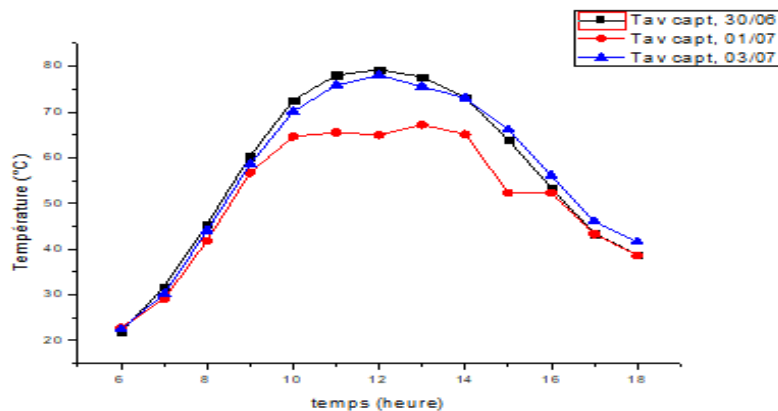


Figure 5: Temperature profile in sensor

### 2.3. Condenser temperature profile

Figure 6 illustrates the evolution of condenser temperature and ambient temperature as a function of time for the three days 30/06, 01/07 and 03/07/2017. It can be seen that the condenser temperature rose faster than the ambient temperature, with maximum values of 48.4°C, 44.4°C and 47°C between 8 and 10 am.

This could be explained by the desorption process. In fact, the desorption process creates a pressure rise that drives the water vapor towards the condenser. The condensation temperature rises progressively as a result of the increase in water vapor temperature during the period from 6h to 14h.

After 2 p.m., the collector temperature falls as solar radiation decreases, leading to a drop in condenser temperature. Under these conditions, the flow of water vapor through the condenser is at its lowest, and is cancelled out when the condenser temperature becomes equivalent to the ambient temperature. This similar trend in condenser temperature evolution was observed experimentally by F. Bouzeffour [3]. But, the evolution of the condensation temperature was represented over the time period from 9 a.m. to 2 p.m. and the maximum temperatures obtained in the condenser ranged from 45°C to 53°C.

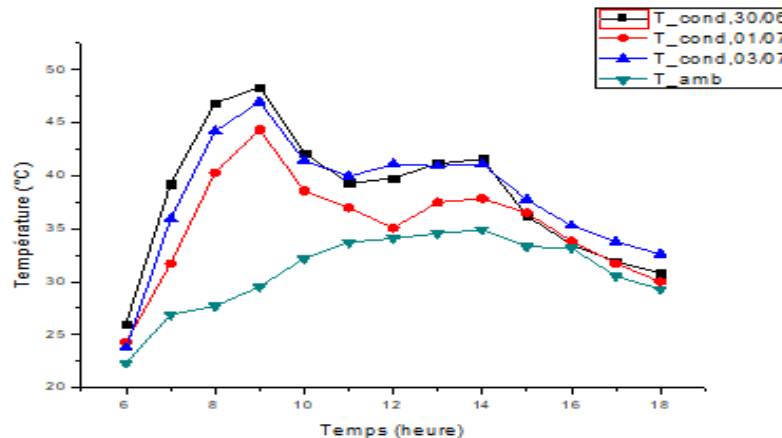


Figure 6 : Condenser temperature profile

### 2.4. Evaporator and storage tank temperature profile

The evaporator temperature profile curves for 06/30, 07/01 and 07/03/2017 are illustrated in Figure 7. This figure illustrates the evolution of evaporator temperature over three days as a function of time. It can be seen that the evaporator temperature increases over the test days to reach a respective maximum value of 16.3°C, 13.37 °C and 13.55 °C at 6 pm. This increase in evaporator temperature is due to the fact that the cold room in the system is not airtight.

Also, after 6 p.m. the evaporator temperature drops to a minimum value of between 9.8°C and 11.8°C on test days. During the evaporation-adsorption phase (from 6 p.m. to 4 a.m.), a certain amount of cold is produced by the evaporation of water at low pressure. It is important

to note that: (i) water vapor adsorption increases with the absorbent's absorption capacity; (ii) cold production in the chamber becomes significant as water vaporization continues. A similar trend was observed by F. Bouzeffour [3]. According to this author, cold production occurs between 4.40 p.m. and 4 a.m. and the temperature obtained in the evaporator is around +6°C. This difference in evaporator temperatures is due to the fact that the cold room in our system is no longer watertight, due to its age (it was manufactured in 1986).

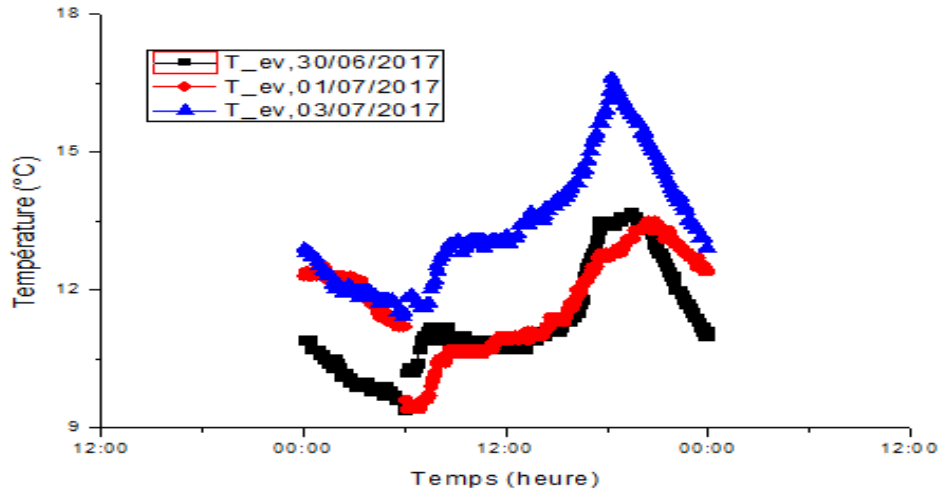


Figure 7: Temperature trends in the cold room

### 2.5. Prototype solar coefficient of performance

Under actual working conditions, with an average condensing temperature  $T_c = 51.3^\circ\text{C}$  and a minimum evaporator temperature  $T_e = 9.4^\circ\text{C}$ , the experimental SCOP of the refrigeration system in this study ranges from 0.058 to 0.127 and the total energy received by the solar collector is between  $14.56 \text{ MJ/m}^2$  and  $18.68 \text{ MJ/m}^2$  as shown in Table 1.

The experimental results obtained in this study, were compared with those found in the literature as shown in Table 2. The SCOP values obtained with our device range from 0.091 to 0.138. These results are comparable with those of other adsorption refrigeration systems using silica gel/water or the activated carbon/methanol (Table 2). These results show that our adsorption system is still working reasonably well. In fact, evaporator temperature increases with SCOP. However, it should be noted, that at the evaporation temperatures obtained ( $T_e \geq 9.4^\circ\text{C}$ ), we can only have cool water.

Table 2: Calculation of experimental SCOP

Date	30/06/2017	01/07/2017	02/07/2017	03/07/2017
$T_{amb}$ (°C)	28,3	29,65	31,65	31,65
$T_e$ (°C)	10,2	9,4	14,1	11,6
$T_c$ (°C)	51,3	46,3	44,6	46
$I$ (W/m <sup>2</sup> )	419	337	456	420
E (kJ)	36194,7	29118,5	39356,9	36303,6
$I_g$ (kJ/m <sup>2</sup> )	18097,3	14559,3	19678,5	18151,8
$I_g$ (W/m <sup>2</sup> )	60,03431	48,08211	64,56189	59,55307
$m_{ad}$ (kg)	1,84485	1,07122	2,20435	1,80885
$Q_f$ (kJ)	4570,7021	2656,0694	5440,528	4475,3683
SCOP	0,126	0,091	0,138	0,123

Table 3: Comparison of the COP<sub>s</sub> of some adsorption solar refrigerators.

Prototype	Couple adsorbant/adsorbat	Surface (m <sup>2</sup> )	SCOP	Energie totale reçue	Références
Present study	Silicagel/eau	2	0,091-0,138	14,56-18,68 MJ/m <sup>2</sup>	-
Boubakri et al. (1992)	AC/méthanol	2	0,12	19,54 MJ/m <sup>2</sup>	[10], [11]
Hilbrand et al. (2005)	AC/méthanol	2	0,09-0,13	19-25 MJ	[10], [12]
Pons et Guilleminot (1986)	AC/méthanol	6	0,10-0,12	16-19 MJ/j	[13]
Hildbrand et al. (2004)	Silicagel/eau	2	0,12-0,23	> 20 MJ/m <sup>2</sup> . j	[13]

## Conclusion

This study has enabled us to review the actual operation of the various components of the adsorption solar refrigerator, and to confirm that they work fairly well despite the weather. The study shows that the prototype has a solar coefficient of performance ranging from 0.091 to 0.138 with a solar radiance ranging from 576.45W/m<sup>2</sup> and 733.38 W/m<sup>2</sup>. This result proves that these types of refrigerators stand better to the test of time. However, the evaporator temperature has risen by around 4°C compared with the initial value, resulting in a higher solar coefficient of performance. In other words, the higher the evaporator temperature, the higher the solar coefficient of performance. This latter result has been proven by several simulation studies, such as those by W. Chekirou [14] and M. A. Djebiret [15].

In addition, this good agreement between our result and those of the literature proves that the correlation of A. Errougani's correlation for estimating the mass of adsorbed water is an alternative solution for systems without a device for measuring condensate mass. Some authors, such as G. C. Tubreoumya [8], have used this correlation to estimate the condensate in order to calculate the amount of cold produced at the evaporator.

## References

- [1] K. Rabhi, A. Chaouki, and H. Ben Bacha, "Simulation en régime dynamique d'un système de réfrigération solaire à adsorption," vol. 17, pp. 541–547, 2014.
- [2] L. P. NOLWENN, "Procédé solaire de production de froid basse température (-28C) par sorption solide-gaz," Université de Perpignan, 2005.
- [3] B. Fatih, "Thème Production du froid solaire par adsorption et analyse de la performance par l'application de l'approche de réseaux de neurones artificiels," université hassiba benbouali de chef, 2017.
- [4] F. Lemmini and A. Errougani, "Experimentation of a solar adsorption refrigerator in Morocco," *Renew. Energy*, vol. 32, no. 15, pp. 2629–2641, 2007.
- [5] A. Boubakri *et al.*, "experimental study of adsorption solar powered ice in agdir (Morocco)- 2. Influence of meteorological parameters," no. 1, pp. 15–21, 1992.
- [6] C. Hildbrand, O. Cherbuin, and J. Mayor, "Réfrigération solaire à adsorption," pp. 1–10, 2005.
- [7] F. Bouzeffour, B. Khelidj, and M. Tahar abbes, "Experimental investigation of a solar adsorption refrigeration system working with silicagel/water pair: A case study for Bou-Ismaïl solar data," *Sol. Energy*, vol. 131, pp. 165–175, 2016.
- [8] G. C. Tubreoumya *et al.*, "Experimental analysis of the operation of a solar adsorption refrigerator under Sahelian climatic conditions : case of Burkina Faso," vol. 6495, no. 11, pp. 148–156, 2017.
- [9] W. Chekirou, "Etude et analyse d'une machine frigorifique solaire à adsorption," Université Mentouri-Constantine, 2008.
- [10] A. ROUAG, "Contribution à l'étude du transfert thermique dans les échangeurs de chaleur des machines frigorifiques à adsorption," Université Mohamed Khider-Biskra, 2017.
- [11] W. CHEKIROU, "ETUDE ET ANALYSE D'UNE MACHINE FRIGORIFIQUE SOLAIRE A ADSORPTION," Université Mentouri-Constantine, 2008.
- [12] F. Buchter, P. Dind, and M. Pons, "An experimental solar-powered adsorptive refrigerator tested in Burkina-Faso," *Int. J. Refrig.*, vol. 26, no. 1, pp. 79–86, 2003.
- [13] P. Goyal, P. Baredar, A. Mittal, and A. R. Siddiqui, "Adsorption refrigeration technology - An overview of theory and its solar energy applications," *Renew. Sustain. Energy Rev.*, vol. 53, pp. 1389–1410, 2016.
- [14] W. Chekirou, A. Chikouche, N. Boukheit, A. Karaali, and S. Phalippou, "Dynamic modelling and simulation of the tubular adsorber of a solid adsorption machine powered by solar energy," *Int. J. Refrig.*, vol. 39, pp. 137–151, 2014.
- [15] M. A. Djebiret, M. Ouali, M. Mokrane, N. Hatraf, and N. K. Merzouk, "Etude Paramétrique d'un Cycle a simple effet d'une Machine Frigorifique d'Adsorption," no. June, 2016.